

**COMPARISON OF SMALL FRESH CRATERS IMAGED UNDER PRIMARY AND SECONDARY ILLUMINATION WITH THE LUNAR RECONNAISSANCE ORBITER CAMERA** A. C. Martin<sup>1</sup>, B. W. Denevi<sup>1</sup>, E. J. Speyerer<sup>2</sup>, A. K. Boyd<sup>2</sup>, H. M. Brown<sup>2</sup>, and M. S. Robinson<sup>2</sup>. <sup>1</sup>Johns Hopkins University Applied Physics Laboratory, Laurel, MD, 20723, USA. <sup>2</sup>School of Earth and Space Exploration, Arizona State University, Tempe, AZ, 85281, USA. (anna.martin@jhuapl.edu)

**Introduction:** Local lighting conditions affect the appearance of the lunar surface and thus their geologic interpretation. While photometric effects are well understood under direct or “primary” illumination conditions, interpreting the geology of lunar permanently shadowed regions (PSRs) is complicated by the fact that PSRs receive no direct illumination, but only diffuse “secondary” illumination, which is light reflected (scattered) from one portion of the surface onto another [1].

To gain a better understanding of how secondary illumination affects the appearance of albedo contrasts, we used the Lunar Reconnaissance Orbiter Camera (LROC) Narrow Angle Camera (NAC) [2] to compare albedo features imaged under primary and secondary illumination conditions. This work explores a collection of long-exposure LROC NAC images of equatorial craters acquired when the floor was in shadow, paired with typical ( $\sim 30^\circ$  phase) NAC images, to aid in the interpretation of images of polar PSRs such as those from the ShadowCam instrument [3] on the Korean Pathfinder Lunar Orbiter [4, 5].

**Methodology:** *LROC NAC Observations of Shadowed Terrain:* We examined five equatorial

craters (McMath A, Lalande A, Healy N, Markov, and Kolhorster) imaged by the LROC NAC at high incidence angles ( $>69^\circ$ ) and longer exposure times ( $>20\times$  longer than typical) to replicate secondary illumination conditions in PSRs. NAC image mosaics were constructed to facilitate comparisons between primary and secondary illumination images using low- and moderate-phase ( $\sim 30^\circ$  and  $60^\circ$ , respectively) primary illumination images. All images were orthorectified and controlled to minimize any image-to-image offset.

*Illumination Modeling:* Knowledge of photometric angles is crucial for comparing and interpreting surface reflectance. Lighting conditions for terrain that receives only secondary illumination, sunlight that is reflected from nearby crater rims and massifs, are distinct from those of a typical scene receiving direct illumination from the Sun, which is essentially a point source. Under primary illumination, each location (pixel) has only a single phase angle, and phase angles vary by only  $\sim 5^\circ$  over the NAC field of view ( $\sim 5$  km). However, under secondary illumination, each pixel receives light from multiple angles. Thus we modified

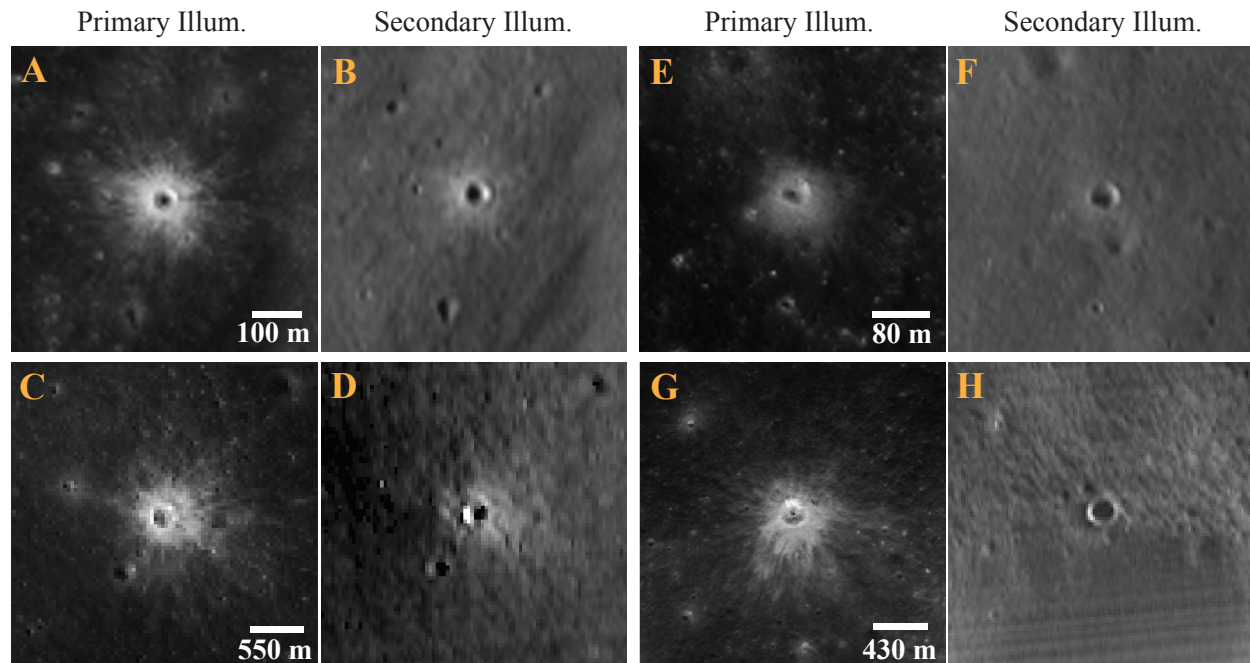


**Figure 1.** Examples of four fresh craters observed in both primary and secondary illumination. The high-reflectance ejecta of small, fresh craters can in some cases be detected in both primary and secondary illumination, such as the examples within McMath A crater (A, B) and Kolhorster crater (C, D). However, in many cases the high-reflectance ejecta of fresh craters observed in primary illumination is not visible in secondary illumination, as seen in other examples within McMath A (E, F) and Healy N craters (G, H).

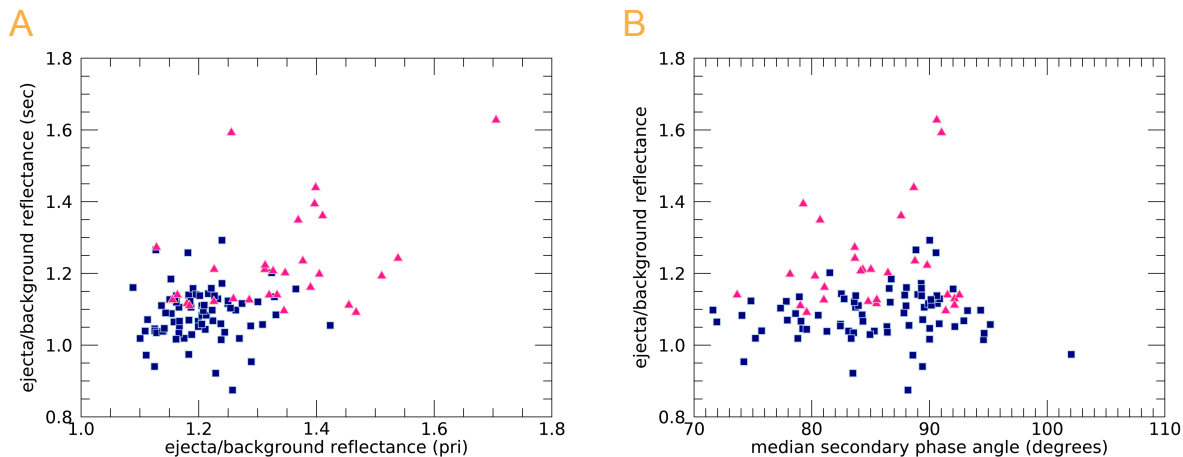


Figure 2. Characteristics of small fresh craters from the combined populations observed in McMath A, Healy N, Markov and Kolhorster. Fresh craters whose high-reflectance ejecta is visible in both primary and secondary illumination are shown as blue squares; where the high-reflectance ejecta is observed in primary illumination but not in secondary illumination is shown as pink triangles. A) The ratio of the reflectance of small crater ejecta to nearby background reflectance is shown for primary and secondary illumination. B) The median secondary phase angle at each location vs. the ejecta/background reflectance ratio in secondary illumination.

the illumination model of Mahanti et al. [6] to record the full range of phase angles at each pixel, weighted by the amount of light contributed from each direction. We then use the median “secondary” phase angle at each pixel, which can vary by  $\sim 20^\circ$  over the NAC field of view, for comparison with secondary reflectance.

**Surface Features:** Using the low-phase primary illumination images, we identified two features of interest, high-reflectance streaks and high-reflectance ejecta deposits from small fresh craters; here we highlight results for the fresh craters. The ejecta deposits of these small craters provide albedo contrasts of high-reflectance ejecta versus the more mature, low-reflectance surroundings. These deposits can be used to understand what level of contrast variations we can expect to detect when imaging PSRs. Because the visibility of high-reflectance deposits is highly dependent on illumination conditions, we mapped the fresh craters twice: first in secondary illumination and then independently in primary illumination ( $\sim 30^\circ$ ); examples are shown in Fig. 1. Craters were mapped in QGIS [7] and any crater with a diameter smaller than  $3\times$  the mapped pixel scale of the secondary illumination image was excluded. The ejecta deposit was defined as extending one crater radius from the rim, while the region between two and three crater radii from the rim was defined as the mature “background” for comparison.

**Results:** We mapped 104 small fresh craters within the interiors of McMath A, Healy N, Markov, and Kolhorster. Overall we noticed that less than a third of these fresh craters ( $n=29$ ; 28%) had high-reflectance ejecta deposits that were detectable in secondary illumination (Fig. 2). Ejecta that has a larger reflectance contrast with the background were more

likely to be identified as fresh craters in secondary illumination. In primary illumination, 73% of the fresh craters that had ejecta  $>30\%$  higher in reflectance than the background was also identifiable as “fresh” in secondary illumination. When the ejecta is  $<30\%$  higher in reflectance than the background, only  $\sim 13\%$  of the fresh craters are identifiable in secondary illumination. For both primary and secondary illumination, all fresh craters detected have a contrast between ejecta and background greater than  $\sim 10\%$ .

While we examined several factors to understand what controls whether or not a fresh crater is identifiable in secondary reflectance, we see no clear relationship between median secondary phase angle (Fig. 2B). The percentage of craters detectable in secondary illumination is approximately the same across all median secondary phase angles and the size and location within their host crater did not seem to have an impact on their visibility. However, we note that few craters are observed at median secondary phase angles  $<80^\circ$  (Fig. 2B), where, based on comparisons with primary illumination phase curves, we would expect reflectance contrasts, due to albedo, to increase. This high degree of local variation in phase angle and resulting visibility of albedo differences highlights the importance of modeling the complex phase angles observed in PSRs, where no images with primary illumination are available for comparison.

**References:** [1] Speyerer et al., 2013, *Icarus*, 222, 122-136. [2] Robinson et al., 2010, *Sp. Sci. Rev.*, 150, 81-124. [3] Robinson et al., 2022, *COSPAR*, Abstract #B3. [4] Kang et al., 2021, *KSAS Conf.*, 404-405. [5] Song et al., 2016, 14th Inter. Conf. Space Op. [6] Mahanti et al., 2022, *IEEE*, 19, 1-4. [7] QGIS.org, 2022. QGIS Geographic Information System. QGIS Association. <http://www.qgis.org>